Incorporation of $Ru_2(O_2C(CH_2)_6CH_3)_4$ into Extended Chains: Interaction of $Ru_2(O_2C(CH_2)_6CH_3)_4$ with Pyrazine, 4-Cyanopyridine, TCNE, and *p*-Benzoquinone

Jodi L. Wesemann[†] and Malcolm H. Chisholm*

Department of Chemistry, Indiana University, Bloomington, Indiana 47405-4001

Received February 14, 1997[⊗]

In attempts to form extended chains $Ru_2(O_2C(CH_2)_6CH_3)_4$ (**1**) was reacted with both simple coordination and redox-active bridging ligands. The simple coordination ligands, pyrazine (pz) and 4-cyanopyridine (4-cp), coordinated in the axial sites of the diruthenium complex. With the symmetric ligand pyrazine, the polymer $[\mathbf{1}(pz)]_n$ was isolated. With the asymmetric ligand 4-cp, the pyridine nitrogen coordinated preferentially and the bis-adduct $\mathbf{1}(4\text{-cp})_2$ was isolated. Solution UV/visible and NMR studies indicated that π-interactions between the Ru−Ru π^* and ligand π orbitals were occurring in both cases. Mole ratio and continuous variation studies of **1** with pyrazine and 4-cp indicated that these axial ligands were labile and that a number of solution species existed. When **1** was reacted with TCNE, redox reactions occurred. Solid-state IR and solution NMR studies also showed that both **1**(TCNE) (**2**) and $[\mathbf{1}]_2$TCNE (**3**) contained diruthenium carboxylate cores which no longer possessed the D_{4h} paddle-wheel geometry. With *p*-benzoquinone, redox reactions occurred upon coordination to give $[\mathbf{1}^+][SQ^{-\bullet}]$ (**4**), which contained an undisrupted oxidized diruthenium tetracarboxylate core. Formation of **4** was reversible in solution, with **1** and *p*-benzoquinone being favored at higher temperatures.

Introduction

Earlier work in our research group has focused on incorporating the quadruply-bonded dimolybdenum and ditungsten carboxylate cores into macromolecular species.[1] The $M_2(O_2CR)_4$ species have a paddle-wheel or lanternlike structure with the carboxylates, which bridge the M−M bond, occupying the equatorial sites. Either solvent molecules or the carboxylate oxygens of neighboring molecules coordinate weakly in the axial sites. Extended systems were formed from $M_2(O_2CR)_4$ (M = Mo, W) by replacing the equatorial carboxylates with bridging ligands such as oxalate, which linked the dinuclear centers together with the M−M quadruple bonds perpendicular to the axis of propagation, or 1,8-anthracenedicarboxylate, which arranged the M−M bonds more or less parallel to the propagation axis. Electronic communication between the group 6 dinuclear units was facilitated by these bridging ligands since they contain π-LUMOs of the appropriate symmetry to interact with the M−M δ HOMOs of the dimetal cores.

Diruthenium carboxylates have M−M π^* HOMOs and must be linked by different ligands if electronic communication is to occur between dinuclear units. Our ^{1}H NMR studies on various bis-adducts of the paramagnetic $Ru_2(O_2CR)_4$ species have shown that the unpaired electrons occupying the Ru−Ru π^* orbitals are directly delocalized into π systems of axial ligands.[2] This suggests that communication could occur between $Ru_2(O_2CR)_4$ units via bridging axial ligands such as the nitrogen-containing bridges shown in Chart 1.

A number of dimetal tetracarboxylates have been linked by axial ligands, resulting in polymeric species.[3−8] In some extended chains the bridging ligands simply coordinate in the axial sites, causing the M−M bonds to be parallel to the axis of propagation. Pyrazine (pz) has been used to link $Cr_2(O_2CCH_3)_4$[3] and $Cu_2(O_2CCH_3)_4$.[4] $Mo_2(O_2CCH_3)_4$ units have been connected by 4,4′-bipyridine,[5] and $Rh_2(O_2CC_2H_5)_4$ by phenazine (phz).[6] Phenazine has also been used to link cationic $Ru_2(O_2CC_2H_5)_4^+$ complexes into polymers.[7] X-ray structures of the above have confirmed that the dimetal tetracarboxylate cores stayed intact, i.e. that no carboxylates were displaced from the equatorial sites and the M−M bond remained. In other extended chains the bridging ligands have the potential to oxidize the $M_2(O_2CR)_4$ species. Although TCNE and the oxygen-containing *p*-benzoquinone did not oxidize dirhodium or dimolybdenum carboxylates, as discussed below, reaction of another redox-active ligand, 2,5-dimethyl-*N*,*N*′-dicyanoquinonediimine (DM-

Chart 1

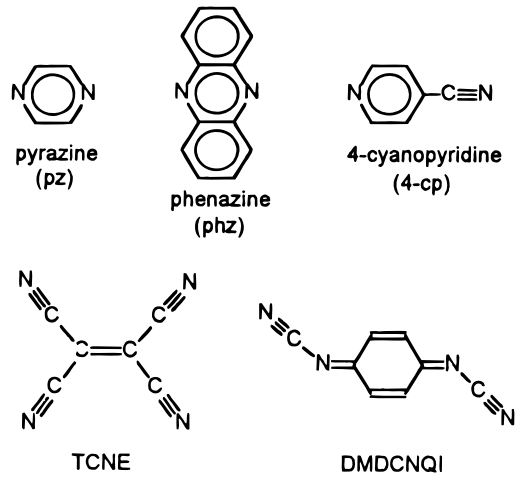

[†] Current Address: Department of Chemistry, Saint Mary's College of California, Moraga, CA 94575.

[⊗] Abstract published in *Advance ACS Abstracts,* June 1, 1997.

(1) (a) Cayton, R. H.; Chisholm, M. H.; Huffman, J. C.; Lobkovsky, E. B. *J. Am. Chem. Soc.* **1991**, *113*, 8709. (b) Cayton, R. H.; Chisholm, M. H. *J. Am. Chem. Soc.* **1989**, *111*, 8921.
(2) Wesemann, J. L.; Chisholm, M. H.; Christou, G.; Folting, K.; Huffman, J. C.; Samuels, J. A.; James, C. A.; Woodruff, W. H. *Inorg. Chem.* **1996**, *35*, 3643.
(3) Cotton, F. A.; Felthouse, T. R. *Inorg. Chem.* **1980**, *19*, 328.
(4) Morosin, B.; Hughes, R. C.; Soos, Z. G. *Acta Crystallogr. B* **1975**, *31*, 762.
(5) Handa, M.; Kasamatsu, K.; Kasuga, K.; Mikuriya, M.; Fujii, T. *Chem. Lett.* **1990**, 1753.
(6) Cotton, F. A.; Felthouse, T. R. *Inorg. Chem.* **1981**, *20*, 600.
(7) Cotton, F. A.; Kim, Y.; Ren, T. *Inorg. Chem.* **1992**, *31*, 2723.
(8) Huckett, S. C.; Arrington, C. A.; Burns, C. J.; Clark, D. L.; Swanson, B. I. *Synth. Met.* **1991**, *42*, 2769.

S0020-1669(97)00173-0 CCC: $14.00

DCNQI), with $Ru_2(O_2CR)_4$ formed a polymer containing oxidized $Ru_2(O_2CR)_4^+$ and reduced $DMDCNQI^-$ units, as determined by EPR and IR studies.[8]

Studies of the polymers mentioned in the previous paragraph have utilized only solid samples and not provided any information on the nature of the solution species. The diruthenium compound used here, $Ru_2(O_2C(CH_2)_6CH_3)_4$ (**1**), contains long-chain carboxylates that enhance solubility, allowing NMR, EPR, UV/visible, and IR solution methods to be used for characterization. The paramagnetism of the diruthenium species makes ^1H NMR spectroscopy most informative, indicating changes in the oxidation state of the diruthenium core, the relative extent of delocalization of unpaired electron density onto ligands, cleavage of the Ru−Ru bond (which has been shown to occur with CO,[9] PPh_3,[9,10] and pyridine[9,11]), and the relative lability of axial ligands.[2] EPR signals also indicate changes in oxidation state, being seen for the cationic $Ru_2(O_2CR)_4^+$ species[12,13] but not for neutral $Ru_2(O_2CR)_4$. Electronic spectra reflect the degree of π interaction between the axial ligand and the Ru−Ru π^* orbitals. On the basis of single-crystal polarized electronic spectra of $Ru_2(O_2CR)_4^+$,[14] the major absorption for **1** is presumed to be due to the Ru−Ru π to Ru−Ru π^* transition. Greater interaction of the Ru−Ru π^* orbitals with the ligand π-system will stabilize the former, shifting the Ru−Ru π to Ru−Ru π^* transition to lower energies. Finally, the coordination modes of ligands may be determined by distinctive ligand stretches in the IR region. Use of these four spectroscopies, as described below, provides insight into the interactions of $Ru_2(O_2CR)_4$ with both the simple coordination ligands, pyrazine and 4-cyanopyridine, and the redox-active ligands, TCNE and *p*-benzoquinone.

Results and Discussion

Pyrazine. Bonding Considerations. Since the initial report of the Creutz−Taube ion $[Ru(NH_3)_5]_2pz^{5+}$,[15] many studies have been carried out on it[16] and other pyrazine-bridged systems.[17] For electronic communication to occur via the bridging ligand, the pyrazine LUMO must interact with metal-based orbitals of the same symmetry[18] and similar energy.[19] The $Ru_2(O_2CR)_4$ species meets both of these criteria, as seen in the molecular orbital diagram in Figure 1, which is based on our extended Hückel MO calculations. The partially occupied Ru−Ru π^* orbital lies less than 1 eV lower in energy than the pyrazine π-LUMO. Since the antibonding interaction between the d orbitals of the two metal centers raises the energy of the Ru−Ru π^* orbital, this energy gap is much smaller than the calculated 1.99 eV gap between the d orbitals in $Ru(NH_3)_5^{2+}$ and the pyrazine LUMO.[20] The antibonding interaction also causes the lobes of the Ru−Ru π^* orbital to be extended towards the axial sites.

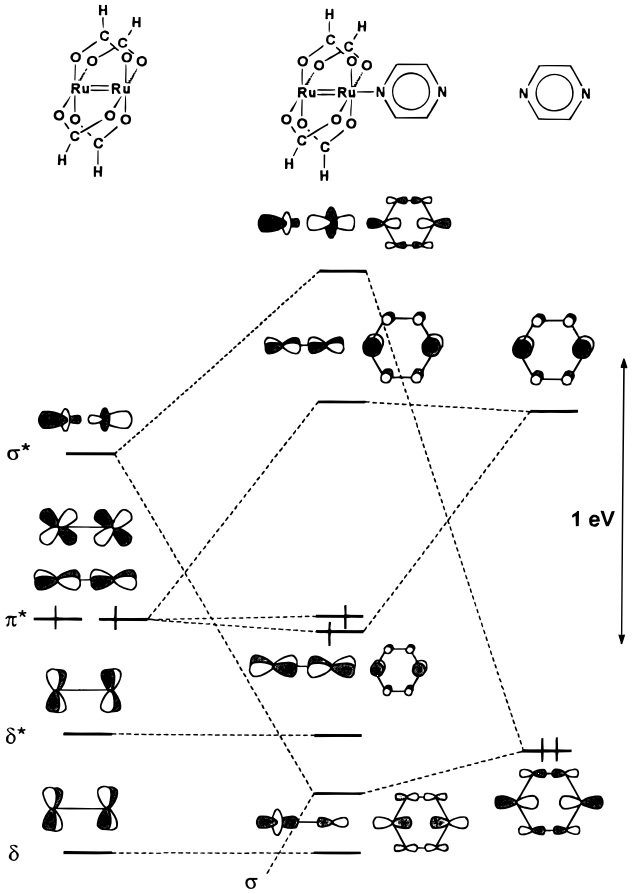

Figure 1. MO diagram showing HOMO/LUMO interactions between $Ru_2(O_2CH)_4$ and pyrazine. The pyrazine HOMO interacts with both the Ru−Ru σ^* and σ orbitals. The antibonding and nonbonding combinations are shown here.

The higher energy of the Ru−Ru π^* orbital and the increased potential for overlap led us to expect a greater degree of interaction with the pyrazine LUMO than our calculation predicted. The small amount of stabilization/destabilization calculated for the $Ru_2(O_2CH)_4$pz interaction is likely due to the rather long Ru−N distance (2.4 Å), which was chosen to correspond to the Ru−N distances (2.436(4) and 2.443(5) Å) in $[Ru_2(O_2CC_2H_5)_4phz)]^+[BF_4]^-$ (phz = phenazine).[7] Consideration of other Ru−N distances suggests that steric interactions with phenazine may cause this distance to be longer than it would be with pyrazine. In $[Ru_2(chp)_4^+]_2pz$ (chp = 6-chloro-2-hydroxypyridinate), Ru−N distances were 2.275(5) Å.[21] The Ru−N distances in $[Ru(NH_3)_5]_2pz^{5+}$ were shorter yet (2.002(2) Å for the chloride and 1.972(4) Å for tosylate salt.)[16] Thus, the Ru−N distances between **1** and pyrazine are probably shorter than 2.4 Å and the π interactions likely enhanced beyond those shown in Figure 1.

The diagram in Figure 1 also indicates the importance of the σ-interaction between the Ru−Ru σ^* LUMO and pyrazine HOMO. As our work with nitriles showed,[2] without a relatively strong σ-interaction, π-acceptor ligands do not bind strongly to $Ru_2(O_2C(CH_2)_6CH_3)_4$ (**1**). Pyrazine, however, forms both σ and

(9) Lindsay, A. J.; Wilkinson, G.; Motevalli, M.; Hursthouse, M. B. *J. Chem. Soc., Dalton Trans.* **1987**, 2723.
(10) Lindner, E.; Fawzi, R.; Hiller, W.; Carvill, A.; McCann, M. *Chem. Ber.* **1991**, *124*, 2691.
(11) Stephenson, T. A.; Wilkinson, G. *J. Inorg. Nucl. Chem.* **1966**, *28*, 2285.
(12) Telser, J.; Drago, R. S. *Inorg. Chem.* **1984**, *23*, 3114.
(13) Cotton, F. A.; Pedersen, E. *Inorg. Chem.* **1975**, *14*, 388.
(14) Miskowski, V. M.; Gray, H. B. *Inorg. Chem.* **1988**, *27*, 2501.
(15) Creutz, C.; Taube, H. *J. Am. Chem. Soc.* **1969**, *91*, 3988.
(16) (a) Creutz, C.; Taube, H. *J. Am. Chem. Soc.* **1973**, *95*, 1086. (b) Furholz, U.; Joss, S.; Bürgi, H. B.; Ludi, A. *Inorg. Chem.* **1985**, *24*, 943. (c) Darriet, J.; Haddad, M. S.; Duesler, E. N.; Hendrickson, D. N. *Inorg. Chem.* **1979**, *18*, 2679. (d) Furholz, U.; Burgi, H.-B.; Wagner, F. E.; Stebler, A; Ammeter, J. H.; Krausz, E.; Clark, R. J. H.; Stead, M. J.; Ludi, A. *J. Am. Chem. Soc.* **1984**, *106*, 121.
(17) (a) Kaim, W. *Angew. Chem., Int. Ed. Engl.* **1983**, *22*, 171. (b) Kobel, W.; Hanack, M. *Inorg. Chem.* **1986**, *25*, 103. (c) Kameke, A. von; Tom, G. M.; Taube, H. *Inorg. Chem.* **1978**, *17*, 1790. (d) Adeyemi, S. A.; Johnson, E. C.; Miller, F. J.; Meyer, T. J. *Inorg. Chem.* **1973**, *12*, 2371. (e) Kubel, F.; Strähle, J. *Z. Naturforsch.* **1981**, *36b*, 441.
(18) (a) Richardson, H. W.; Wasson, J. R.; Hatfield, W. E. *Inorg. Chem.* **1977**, *16*, 484. (b) Haddad, M. S.; Hendrickson, D. N.; Cannady, J. P.; Drago, R. S.; Bieksza, D. S. *J. Am. Chem. Soc.* **1979**, *101*, 898. (c) Reference 16 c.
(19) Johnson, C. R.; Shepherd, R. E. *Inorg. Chem.* **1983**, *22*, 2439.
(20) Lavallee, D. K.; Fleischer, E. B. *J. Am. Chem. Soc.* **1972**, *94*, 2583.
(21) Cotton, F. A.; Kim, Y.; Ren, T. *Inorg. Chem.* **1992**, *31*, 2608.

Table 1. UV/Visible Data for **1** and [**1**(pz)]$_n$

	λ_{max} nm ($\epsilon \times 10^{-3}$ M^{-1} cm^{-1})	
solvent	**1**	[**1**(pz)]$_n$
toluene[a]	462 (1.10)	488 (2.44)
THF	442 (0.97)	442 (1.15)
MeOH	438 (0.72)	434 (0.97)

[a] At 3.2×10^{-4} M.

π bonding interactions with **1**, forming the bis-adduct in solution when 2 equiv of the ligand is present.

Preparation and Characterization of [1(pz)]$_n$. Pyrazine also formed bridges between diruthenium tetracarboxylates. Reactions of brown toluene solutions of **1** with pyrazine in a 1:1 molar ratio resulted immediately in intensely-colored purple solutions, from which purple powder precipitated over time.[22] The precipitate analyzed as expected for [$Ru_2(O_2C(CH_2)_6CH_3)_4$-pz]$_n$ ([**1**(pz)]$_n$). While we were carrying out solution studies on [**1**(pz)]$_n$, an analogous polymer [$Ru_2(O_2C(CH_2)_{10}CH_3)_4$pz]$_n$ was reported.[23] Synthesized in hot ethanol, it precipitated immediately, giving a purple product with characterization data similar to [**1**(pz)]$_n$. Solid-state IR spectra of [**1**(pz)]$_n$ showed the stretches for the bridging carboxylate ligands, $\nu_{asym}(O_2C)$ and $\nu_{sym}(O_2C)$, at 1551 and 1424 cm^{-1}, respectively (compared to 1560 and 1430 cm^{-1} for the dodecanoate derivative[23]), shifted from 1545 and 1415 cm^{-1} for **1**. Thus, the dimeric core was affected by pyrazine coordination but not cleaved. (Related monomeric species that were synthesized from **1** showed monodentate carboxylate stretches at ca. 1600 cm^{-1}.) Additional IR bands seen at 1041, 1126, and 3050 cm^{-1} were attributed to the pyrazine ligand. The out-of-plane CH bending mode, affected by metal coordination,[24] was shifted from 790 cm^{-1} for free pyrazine to 815 cm^{-1} for [**1**(pz)]$_n$ and was one of those shifted when pyrazine-d_4 was used, supporting its assignment as a C−H mode. The pyrazine centrosymmetric stretch at 1580 cm^{-1}, the in-plane C−H bend at 1230 cm^{-1}, and the ring deformation at 695 cm^{-1} were not seen, indicative of bridging pyrazine.[25]

Unlike the dodecanoate species, which was reported to be insoluble in common solvents,[23] [**1**(pz)]$_n$ dissolved in both noncoordinating and coordinating solvents. This allowed us to study the stability of the polymer in solution. The coordinating solvents were sources of additional axial ligands, alleviating the need for pyrazine to bridge two axial sites. These solvents, however, did not preclude pyrazine from binding or from forming [**1**(pz)]$_n$ films. In noncoordinating solvents, the polymer did not dissociate, but its length was dependent on the solution concentration. These observations and our studies on solutions of various **1**:pz ratios indicated dynamic solution behavior.

Solution Studies of [1(pz)]$_n$ in Coordinating Solvents. Dissolution of [**1**(pz)]$_n$ in coordinating solvents, such as THF and methanol, resulted in the disappearance of the purple color caused by the bridging pyrazine ligand. Although the extended chain was broken, pyrazine was still interacting with the $Ru_2(O_2CR)_4$ unit. UV/visible data (Table 1) showed that the molar absorptivities of [**1**(pz)]$_n$ in coordinating solvents were ca. 200 M^{-1} cm^{-1} higher than those of **1** (even though λ_{max} values were similar), suggesting that a π-interaction with pyrazine caused the MO containing the Ru−Ru π^* orbital to possess more ligand character and, thus, the Ru−Ru π to Ru−Ru π^* transition to be less forbidden.

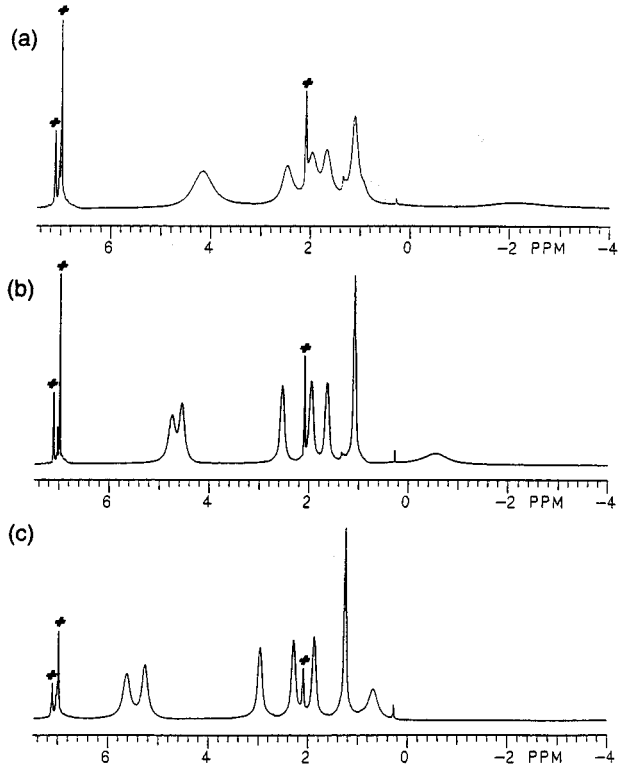

Figure 2. ^{1}H NMR spectra of **1**:pz in (a) 2:1, (b) 1:1, and (c) 1:2 ratios in toluene-d_8. The resonances indicated by an asterisk arise from protio impurities in the solvent.

VT ^{1}H NMR solution studies showed that the axially-bound pyrazine ligands underwent exchange with coordinating solvents. The ^{1}H NMR spectrum of [**1**(pz)]$_n$ in THF-d_8 at room temperature showed no free pyrazine signals. The carboxylate signals were less resolved than those seen for **1**[2] and broadened upon cooling. At −18 °C, several sets of signals were seen, one corresponding to **1**(THF)$_2$. The presence of only a low intensity signal for uncoordinated pyrazine suggested that **1**(pz)$_2$ was the other major product, with a small amount of **1**(THF)(pz) present. A small signal at −60 ppm, in the region for axial ligands yet further upfield than for the nonbridging pyrazine, suggested that a fourth species involving bridging pyrazine was also present in solution. Addition of several equivalents of pyrazine caused the relative ratios of the ^{1}H NMR signals to shift. When a large excess (50 equiv) was added, the dimer was cleaved within several hours and the ^{1}H NMR spectrum showed only diamagnetic species. Despite the number of species formed, only [**1**(pz)]$_n$ was isolated as a solid from THF solutions of **1** with various ratios of pyrazine.

Solution Studies of [1(pz)]$_n$ in Noncoordinating Solvents. In aromatic solvents, the extended chain was maintained. [**1**(pz)]$_n$ dissolved in toluene or benzene, upon heating, to form purple solutions. Figure 2 shows the effect of different **1**:pz ratios on room-temperature ^{1}H NMR spectra. Due to the coordination of pyrazine to the $Ru_2(O_2CR)_4$ unit, the ^{1}H NMR spectrum in toluene-d_8 at room temperature (Figure 2b) was significantly different than the broad unresolved signals of **1**[2] (which maintains its axial M--O interactions in benzene). The ^{2}H NMR spectrum of [**1**(pz-d_4)]$_n$, which showed only one pyrazine signal at −37 ppm, is consistent with the presence of a bridging pyrazine ligand.

The UV/visible spectrum of [**1**(pz)]$_n$ in toluene showed a concentration dependent absorption at ca. 490 nm with a

(22) Similar products (R = H, Me, Et, CCF_3, CMe_3, and Ph) have been synthesized but were insoluble: Zozulin, A. J.; Clark, D. L.; Burns, C. J.; Sattelberger, A. P.; Swanson, B. I., private communication.

(23) Bonnet, L.; Cukiernik, F. D.; Maldivi, P.; Giroud-Godquin, A.-M.; Marchon, J.-C.; Ibn-Elhaj, M.; Guillon, D.; Skoulios, A. *Chem. Mater.* **1994**, *6*, 31.
(24) Kubel, F.; Strähle, J. *Z. Naturforsch.* **1981**, *36b*, 441.
(25) Metz, J.; Schneider, O.; Hanack, M. *Spectrochim. Acta* **1982**, *38A*, 1265.

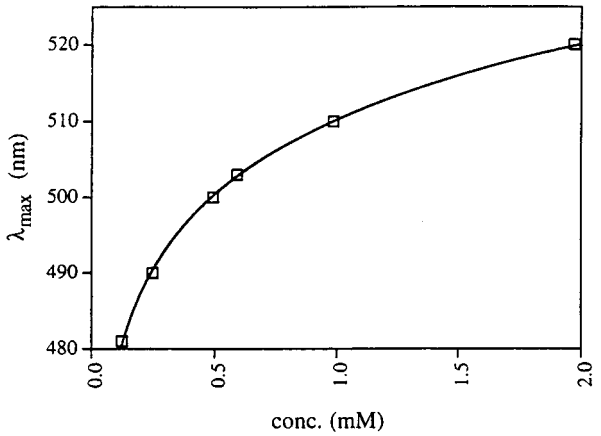

Figure 3. Dependence of λ_{max} for the Ru−Ru $\pi \rightarrow \pi^*$ transition on concentration of $[\mathbf{1}(pz)]_n$.

Scheme 1

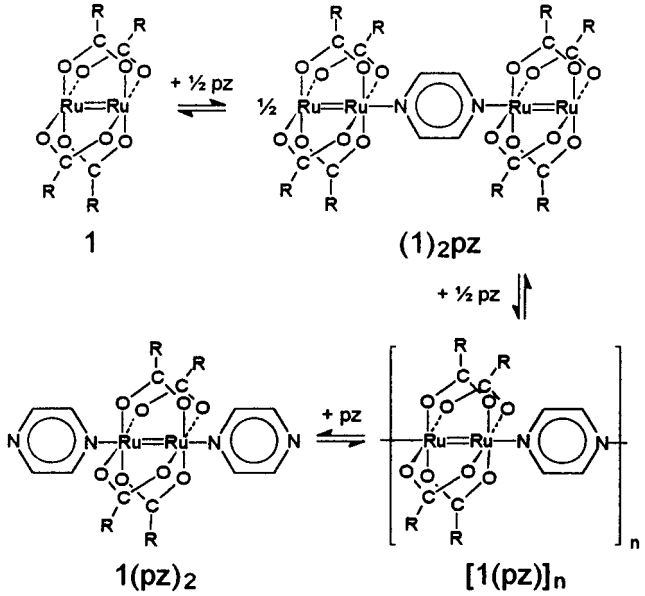

shoulder at ca. 600 nm. A stabilizing interaction between the Ru−Ru π^* HOMO and the pyrazine LUMO (Figure 1) causes the Ru−Ru $\pi \rightarrow$ Ru−Ru π^* absorption seen at 460 nm for **1** to shift to 490 nm for $[\mathbf{1}(pz)]_n$. Increased ligand character of the metal-based π^* orbital explains the observed increase in molar absorptivity. The concentration dependence of λ_{max} for the metal-based $\pi \rightarrow \pi^*$ absorption (Figure 3), which shifts from 480 to 520 nm over a range of 1.2×10^{-4} to 2.0×10^{-3} M, is typical for extended π-systems which increase in length at higher concentrations,[26] supporting the presence of $[\mathbf{1}(pz)]_n$ in solution. Upon prolonged standing, longer chains formed in the toluene solutions, depositing as insoluble purple/black films and hampering attempts to determine the degree of oligomerization in solution.

Variation of 1:pz Stoichiometry. ^{1}H NMR and UV/visible studies in noncoordinating solvents indicated that the species present in solution depended upon the relative pyrazine concentration, as shown by the series of equilibria in Scheme 1. Low-temperature studies led to precipitation however, preventing any information on equilibrium species from being gained. UV/visible titrations of **1** in toluene with pyrazine (Figure 4) indicated that the metal-based $\pi \rightarrow \pi^*$ absorption shifted from 462 nm, for **1** without pyrazine, to 510 nm, with $^1/_2$ equiv of

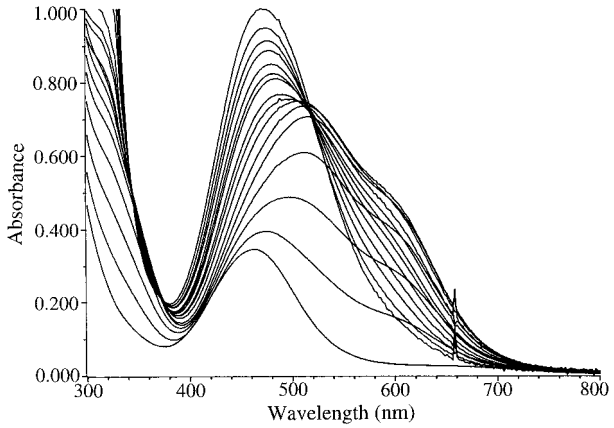

Figure 4. UV/visible spectra from the titration of **1** with pz in toluene. All spectra are for solutions 3.2×10^{-4} M in **1**. The spectrum for the 1:1 ratio corresponds to that of $[\mathbf{1}(pz)]_n$. The spike at 660 nm is an instrumental artifact.

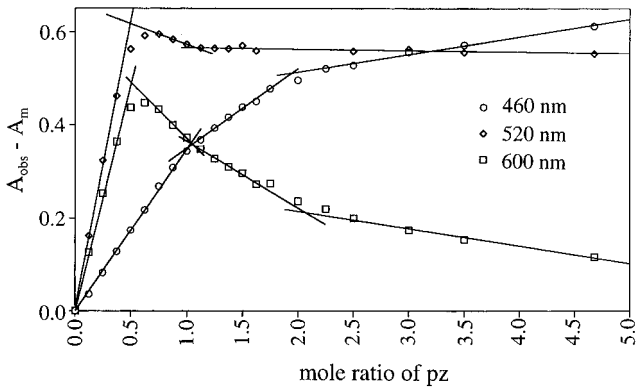

Figure 5. Plot of $A_{obs} - A_M$ vs mole ratio of pyrazine for **1** and pyrazine.

pyrazine, and back to 472 nm, with excess pyrazine. The spectrum for the solution containing **1** and pyrazine in a 1:1 ratio corresponded to that of isolated $[\mathbf{1}(pz)]_n$.

Mole ratio plots[27b] were used to determine the number (three) and stoichiometry ($(\mathbf{1})_2pz$, $[\mathbf{1}(pz)]_n$, $\mathbf{1}(pz)_2$) of the pyrazine adducts in solution. The corrected absorbances, $A_{obs} - A_m$, where A_{obs} is the observed absorbance and A_m is the absorbance for **1** without pyrazine, were plotted vs the mole ratio of pyrazine (Figure 5). When only one stable complex is formed, such mole ratio plots simply show two straight lines intersecting at the mole ratio of the complex.[27b] The absorbances, monitored at 460, 520 and 600 nm, suggest that at least three pyrazine adducts are formed, most likely those shown in Scheme 1. The intersections at $x = 0.5$ for 520 and 600 nm are consistent with the formation of a pyrazine-bridged "dimer-of-dimers", $(\mathbf{1})_2pz$. The lack of intersection for 460 nm at $x = 0.5$ is attributed to the similar molar absorptivities of **1** and $(\mathbf{1})_2pz$ at this wavelength. Intersections at $x = 1$ were seen for all three wavelengths, indicating that $[\mathbf{1}(pz)]_n$ was present. Intersections at $x = 2$ support the presence of the bis-adduct $\mathbf{1}(pz)_2$. Essentially identical molar absorptivity for $[\mathbf{1}(pz)]_n$ and $\mathbf{1}(pz)_2$ (indicated by the isosbestic point at 520 nm in Figure 4) and deviation of the data prevented this intersection from being seen in the 520 nm plot.

The method of continuous variations[27] confirmed the existence of more than one pyrazine adduct in solution. UV/visible spectra of various ratios of isomolar solutions of **1** and pyrazine

(26) (a) Fox, M. A. *Acc. Chem. Res.* **1992**, *25*, 569. (b) Stoner, T. C.; Geib, S. J.; Hopkins, M. D. *J. Am. Chem. Soc.* **1992**, *114*, 4201.

(27) (a) Vosburgh, W. C.; Cooper, G. R. *J. Am. Chem. Soc.* **1941**, *63*, 437. (b) Beck, M. T.; Nagypál, I. *Chemistry of Complex Equilibria*; John Wiley and Sons: New York, 1990; pp 112−120.

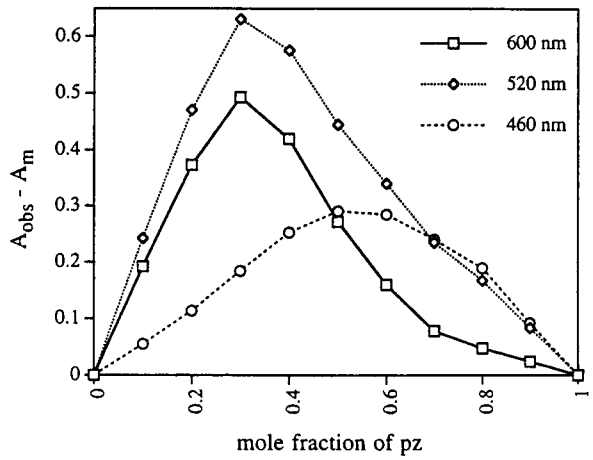

Figure 6. Plot of $A_{obs} - A_M$ vs mole fraction of pyrazine for **1** and pyrazine.

were collected. The difference $A_{obs} - A_m$ (here A_m was calculated for each mixture on the basis of the concentration of **1**) was plotted vs the mole fraction of pyrazine (Figure 6). Although the absorbances at 460 nm reached a maximum near a mole fraction of 0.5, as would be expected for a 1:1 species, the maximum absorbances at other wavelengths did not, indicating that species of other ratios were present. The overlapping spectra did not have the relationships necessary for rigorously determining the stoichiometry of the other species by this method. However, the absorbance at 600 nm reached a maximum for the 2:1 ratio (Figure 4) suggesting that the presence of bridging pyrazine ligands is responsible for this absorbance. Correspondingly, monitoring absorbances at 600 nm (Figure 6) showed a maximum around 0.33, as did those at 520 nm. These studies lead us to suggest that the pyrazine-bridged "dimer of dimers", $(\mathbf{1})_2$pz, is kinetically persistent in solution. The convex curves for the 600 and 520 nm data in the continuous variations plot (above $x = 0.3$) emphasized that a complex series of equilibria was occurring. None of the absorbances monitored in the method of continuous variations showed a maximum at $x = 0.667$, which would be indicative of a 1:2 species in solution, but this is expected since the absorbance for the 1:2 species was not well separated from the others.

Since the spectra of all the species involved in the equilibria in Scheme 1 do not differ significantly, only the occurrence of the final equilibrium (eq 1) was confirmed by an isosbestic point

$$(1/n)[Ru_2(O_2CR)_4(pz)]_n + pz \rightleftharpoons Ru_2(O_2CR)_4(pz)_2 \quad (1)$$

(at 520 nm). This equilibrium was quickly established, since samples with a 1:2 ratio did not change significantly over time. Addition of excess pyrazine then shifted the equilibrium in eq 1 to the right. The occurrence of this equilibrium and the decreased solubility of $[\mathbf{1}(pz)]_n$ explains why $\mathbf{1}(pz)_2$ could never be isolated from solutions of excess pyrazine. (Note that large excesses of pyrazine were avoided since ^{1}H NMR studies showed that 50 equiv of pyrazine cleaved the dinuclear species.)

Thermal Studies of $[\mathbf{1}(pz)]_n$. The pyrazine bridges were also labile in the solid state. When heated, $[\mathbf{1}(pz)]_n$ lost pyrazine to re-form **1**. A series of subsequent differential scanning calorimetry (DSC) scans showed two transitions, 62 and 73 °C, believed to be solid-solid transitions on the basis of visual observation of $[\mathbf{1}(pz)]_n$ in a melting point apparatus. These transitions were repeatable until the sample was heated above 140 °C. At 191 °C, an endotherm corresponding to loss of pyrazine was seen. The following scan was comparable to those for **1**, with a solid-to-liquid crystal transition occurring at 108 °C. A similar loss of pyrazine was reported for $[Cu_2(O_2CR)_4pz]_n$ species above 150 °C.[28] Thus, the π-interactions occurring in $[\mathbf{1}(pz)]_n$ are not sufficient to maintain the polymeric structure at elevated temperatures.

Table 2. ^{1}H NMR Data for Axial Pyridine Ligands in $\mathbf{1}(L)_2$[a]

L	2-H (ppm)	3-H (ppm)
4-cp	−51	−1.0
pyridine	−47	−1.7
4-picoline	−47	−1.8

[a] In toluene-d_8 at −58 °C.

4-Cyanopyridine. Although reactions of **1** with 4-cyanopyridine (4-cp) were expected to give asymmetrically-bridged species such as those seen with monomeric metal complexes,[29] the only product isolated from reactions of various stoichiometries was $\mathbf{1}(4\text{-cp})_2$. The following data show that 4-cp coordinates as a pyridine rather than as a nitrile ligand. First, the ^{1}H NMR signals for the pyridine protons of $\mathbf{1}(4\text{-cp})_2$ were at chemical shifts similar to those of $\mathbf{1}(py)_2$ (Table 2). Coordination as a nitrile would have increased the distance between the pyridine protons and the paramagnetic metal centers, causing less of a paramagnetic shift. Second, the C≡N stretch of $\mathbf{1}(4\text{-cp})_2$ in the IR spectrum was essentially unchanged from free 4-cp. Finally, the fact that excess 4-cp, like excess pyridine, led to cleavage of the Ru−Ru bond indicated that the pyridine nitrogen was binding in the axial site.

The presence of the electron-withdrawing group in $\mathbf{1}(4\text{-cp})_2$ lowers the energy of the pyridine π^* orbital,[30] favoring interactions with the Ru−Ru π^* orbital. Correspondingly, the metal-based $\pi \rightarrow \pi^*$ absorption for $\mathbf{1}(4\text{-cp})_2$ (502 nm, 3.66×10^{-3} M^{-1} cm^{-1}) occurred at a lower energy and had a higher molar absorptivity than that for $\mathbf{1}(py)_2$ (450 nm, 1.54×10^{-3} M^{-1} cm^{-1}).[2] The ^{1}H NMR data in Table 2 show that for $\mathbf{1}(4\text{-cp})_2$ the cyanopyridine 2-H signal was shifted slightly further upfield and the 3-H signal further downfield than those seen for $\mathbf{1}(py)_2$ and $\mathbf{1}(4\text{-pic})_2$, (4-pic = 4-picoline).[2] Thus, π-delocalization onto the pyrazine ring was enhanced by the presence of the cyano group. Solid-state IR spectroscopic studies showed that the C≡N stretch of 4-cp shifted from 2244 cm^{-1} for free 4-cp to 2238 cm^{-1} for $\mathbf{1}(4\text{-cp})_2$. While the small difference indicates that 4-cp binds to **1** via the pyridine ring, the fact that a shift was observed suggests that π-interactions are occurring between the C≡N group and the diruthenium species via the pyridine ring. Linking $\mathbf{1}(4\text{-cp})_2$ with appropriate metal complexes could lead to polymers with extended π-systems.

Solutions with less than 2 equiv of 4-cp appear to contain additional 4-cp adducts. The UV/visible titration of **1** with 4-cp (Figure 7) showed none of the drastic shifts or new absorptions seen for the pyrazine system. Yet, as 4-cp was added to **1** in toluene, the metal-based $\pi \rightarrow \pi^*$ absorption broadened, λ_{max} shifted to slightly longer wavelengths, and the molar absorptivity increased, suggesting that an equilibrium was being shifted. The UV/visible spectrum for the 1:2 ratio showed λ_{max} at 500 nm, corresponding to the spectrum seen for isolated $\mathbf{1}(4\text{-cp})_2$. This indicated that the equilibrium with 4-cp was readily established.

Analyzing the UV/visible data graphically showed that the equilibrium process involved more than one 4-cp adduct. Since the spectra in Figure 7 are very similar, the mole ratio plot[27b]

(28) Attard, G. S.; Cullum, P. R. *Liq. Cryst.* **1990**, *8*, 299.
(29) (a) Cutin, E. H.; Katz, N. E. *Polyhedron* **1991**, *10*, 653. (b) Katz, N. E.; Creutz, C.; Sutin, N. *Inorg. Chem.* **1988**, *27*, 1687. (c) Cutin, E. H.; Katz, N. E. *Polyhedron* **1987**, *6*, 159. (d) Richardson, D. E.; Taube, H. *J. Am. Chem. Soc.* **1983**, *105*, 40.
(30) Ford, P. C. *Coord. Chem. Rev.* **1970**, *5*, 75.

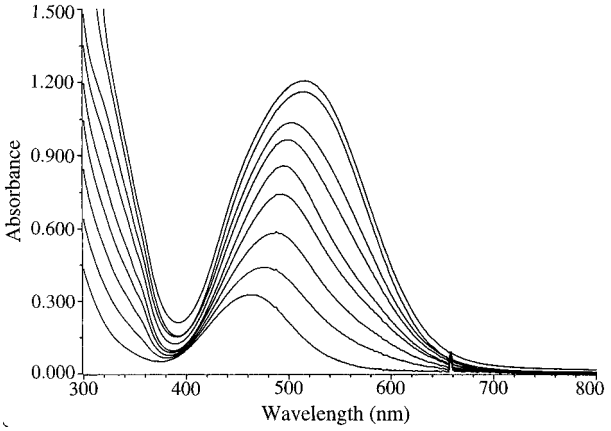

Figure 7. UV/visible spectra from the titration of **1** with 4-cp in toluene. All spectra are for solutions 3.2×10^{-4} M in **1**. The spike at 660 nm is an instrumental artifact.

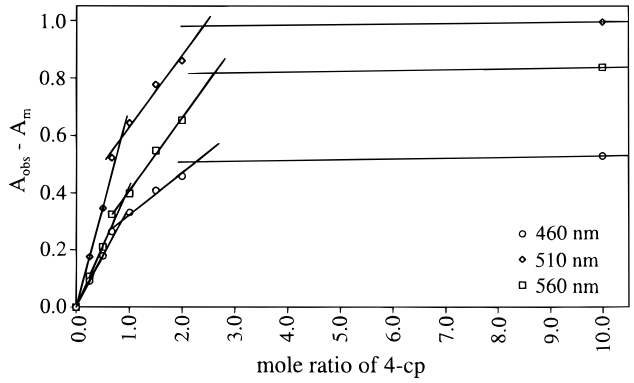

Figure 8. Plot of $A_{obs} - A_M$ vs mole ratio of 4-cp for **1** and 4-cp. An additional data point at a mole ratio of 30 is not shown.

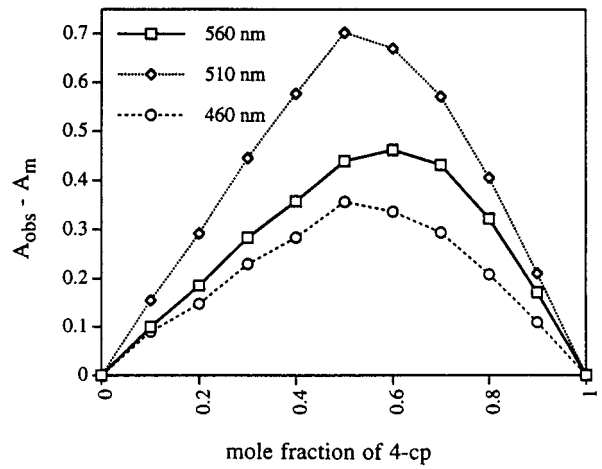

Figure 9. Plot of $A_{obs} - A_M$ vs mole fraction of 4-cp for **1** and 4-cp.

with 4-cp (Figure 8) does not show distinct regions of different slope and the exact stoichiometry of the 4-cp adducts present could not be determined. The data clearly indicated, however, that **1**(4-cp)$_2$ was not the only adduct in solution. Fitting the data with only two lines gave intersections at ca. 1.5, corresponding to **(1)$_2$**(4-cp)$_3$. Fitting with three lines gave intersections at $x = 1$ and $x = 2$, which correspond to **1**(4-cp) and **1**(4-cp)$_2$.

Use of the method of continuous variations[27] (Figure 9) confirmed that **1**(4-cp)$_2$ was not the only adduct in solution. For none of the wavelengths monitored was there a maximum absorbance at a mole fraction of 0.667, while all the wavelengths should have had this maximum if the bis-adduct was the only adduct formed. The maximum values observed varied between mole fractions of 0.5 and 0.6. Without enough pyridine nitrogens to coordinate in both axial sites of **1** either 4-cp also coordinates as a nitrile or the axial sites are filled by the carboxylate oxygens of other diruthenium tetraoctanoates.

Although coordination of benzonitrile to **1** occurred only at low temperatures or with excess nitrile,[2] the pyridine ring in 4-cp was expected to enhance C≡N binding by lowering the π^* orbital based on the C≡N moiety, favoring π-interactions. We attempted to find IR evidence for coordination of 4-cp via C≡N, but studies of dichloromethane solutions of various **1**:4-cp ratios did not indicate that 4-cp was coordinating in this manner, even when less than 2 equiv of 4-cp was present. The C≡N stretch was seen at 2240 cm^{-1} for 0:1, 1:1, and 1:2 ratios of **1**:4-cp. If any 4-cp ligands were bound via C≡N, their stretches were either of very low intensity or shifted under the solvent signals and not observed in our solution IR studies. Apparently coordination of the pyridine group to **1** and the resulting back-bonding raises the energy of the C≡N-based π^* orbital, decreasing any interactions with **1** and explaining why the **1**(4-cp)$_2$ adduct could be isolated but polymeric [**1**(4-cp)]$_n$ could not.

Redox-Active Ligands. In order to synthesize polymeric species whose bridging ligands would be less labile, we investigated redox-active ligands. Such ligands, if their redox potentials are appropriate, will oxidize $Ru_2(O_2CR)_4$ to $Ru_2(O_2CR)_4^+$, the more stable species.[11,31] We anticipated that the reduced ligand would then link the cationic complexes together via their axial sites and coulombic attraction would prevent the ready dissociation seen above.

TCNE. The extended π-system and oxidizing potential of tetracyanoethylene (TCNE) has led to its incorporation in many stacked, charge-transfer salts.[32] In this case, however, we expected TCNE to act as a N-donor ligand, as seen in other transition-metal compounds. The polymeric $[Cu(hfacac)_2TCNE]_n$ (hfacac = hexafluoroacetylacetonate) contains neutral TCNE bridges,[33] while anionic $TCNE^{2-}$ links the iridium units in $[(Ph_3P)_2(OC)Ir]_2TCNE$.[34] Both *trans*-1,2- and 1,1-TCNE bridges have been reported for $[Rh_2(O_2CCH_3)_4TCNE]_n$.[35] TCNE may bridge up to four metal species, as seen in $\{[Rh_2(O_2CCF_3)_4]_2TCNE\}_n$.[36] For these species the oxidation state and bridging mode of the TCNE ligand were determined crystallographically. The oxidation states are reflected in the values for the C≡N stretches in the IR spectra, as shown in Table 3.

The reaction of $Rh_2(O_2CR)_4$ systems with TCNE[35,36] is of particular relevance to the work reported here. Since dirhodium tetracarboxylates are very difficult to oxidize,[37] redox does not occur in the presence of TCNE. With the lack of coulombic attraction and the very labile axial sites,[38] one might expect the neutral TCNE to behave similarily to nitriles, coordinating only weakly and having minimal π-interactions. Yet the C≡N

(31) Bennett, M. J.; Caulton, K. G.; Cotton, F. A. *Inorg. Chem.* **1969**, *8*, 1.
(32) (a) Miller, J. S.; Calabrese, J. C.; Rommelmann, H.; Chittipeddi, S. R.; Zhang, J. H.; Reiff, W. M.; Epstein, A. J. *J. Am. Chem. Soc.* **1987**, *109*, 769. (b) Dixon, D. A.; Miller, J. S. *J. Am. Chem. Soc.* **1987**, *109*, 3656.
(33) Bunn, A. G.; Carroll, P. J.; Wayland, B. B. *Inorg. Chem.* **1992**, *31*, 1297.
(34) Yee, G. T.; Calabrese, J. C.; Vazquez, C.; Miller, J. S. *Inorg. Chem.* **1993**, *32*, 377.
(35) Cotton, F. A.; Kim, Y. *J. Am. Chem. Soc.* **1993**, *115*, 8511.
(36) Cotton, F. A.; Kim, Y. *Inorg. Chim. Acta* **1994**, *221*, 1.
(37) (a) Drago, R. S.; Tanner, S. P.; Richman, R. M.; Long, J. R. *J. Am. Chem. Soc.* **1979**, *101*, 2897. (b) Cannon, R. D.; Powell, D. B.; Sarawek, K.; Stillman, J. S. *J. Chem. Soc., Chem. Commun.* **1976**, 31. (c) Wilson, C. R.; Taube, H. *Inorg. Chem.* **1975**, *14*, 2276.
(38) Felthouse, T. R. *Prog. Inorg. Chem.* **1982**, *29*, 73.

Table 3. ν(C≡N) for Various TCNE Compounds

TCNE charge	compd	ν(C≡N) (cm^{-1})			ref
0	TCNE	2263	2228	2215	
0	$[Cu(hfacac)_2TCNE]_n$	2262	2252	2220	33
0	$\{[Rh_2(O_2CCF_3)_4]_2TCNE\}_n$	2230	2210		35
−1	**2**	2247	2234	2224	
−1	**3**	2228	2220	2206	
−1	KTCNE	2210	2172		
−1	$Mn(CO)_2(Cp^*)TCNE$	2230	2205	2125	53
−1	MnTTP[TCNE][a]	2187	2139	2126	54
−2	Na_2TCNE	2160	2095		55
−2	$[Ir(CO)(PPh_3)_2]_2TCNE$	2176	2097		34

[a] TTP = *meso*-tetraphenylporphyrin.

stretches for the bridging μ_4-TCNE ligand in $\{[Rh_2(O_2CCF_3)_4]_2$-$TCNE\}_n$ are of much lower energy than those for free TCNE or $[Cu(hfacac)_2TCNE]_n$ (Table 3). This indicates that back-donation from the Rh−Rh π^* orbital into the TCNE π-system is occurring. Comparable Rh−N and TCNE distances and color are seen for the acetate-containing derivative *trans*-1,2-$[Rh_2(O_2$-$CCH_3)_4TCNE]_n$.[35] Back-donation may also enhance the bridging ability of TCNE, favoring formation of the polymeric network despite the lack of redox reactivity. The occurrence of π interactions with $Rh_2(O_2CR)_4$ suggests that TCNE might form π-interactions with $Ru_2(O_2CR)_4$ as well.

As the solid-state and solution studies described below indicate, the reaction of **1** with TCNE does result in the expected redox chemistry but does not lead to the anticipated axially-coordinated species. Spectroscopic data lead us to propose the structure **I**, where TCNE has presumably migrated from an axial

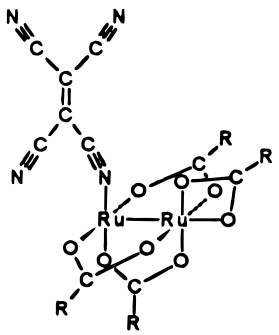

I

to an equatorial site, displacing one bridging equatorial carboxylate ligand. Although dirhodium, dimolybdenum, and ditungsten carboxylate species where axial phosphine ligands have migrated to equatorial sites without cleaving the metal−metal bond have been isolated,[39−41] the maintenance of the Ru−Ru bond with axial ligand migration is unprecedented. With the ligands CO, PPh_3, pyridine, and isocyanide the Ru−Ru bond is cleaved to form diamagnetic $Ru(O_2CR)_2L_x$ (x = 2, 4) products.[9−11] Monomeric products were also reported from the reaction of $Ru_2(O_2CR)_4Cl$ with pyridine[11] and *tert*-butyl isocyanide.[42] Thus, the TCNE adduct is of interest. Unfortunately, even use of shorter chain diruthenium tetracarboxylates did not allow us to confirm our proposed structure using single-crystal X-ray studies.

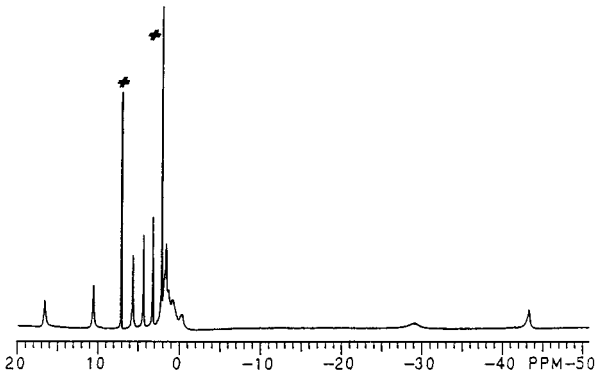

Figure 10. ^{1}H NMR spectrum of **1**(TCNE) (**2**) in toluene-d_8. The resonances indicated by an asterisk arise from protio impurities in the solvent.

TCNE reacted immediately with **1**, forming intense red solutions. A reaction stoichiometry of 1:1 formed $Ru_2(O_2C(CH_2)_6CH_3)_4TCNE$ (**2**), which was soluble in toluene and isolated by addition of hexanes. Elemental analysis of the precipitate was consistent with the 1:1 reaction stoichiometry. The presence of $\mathbf{1}^+$ and $TCNE^{-\bullet}$ indicated that a one-electron redox reaction had occurred. ^{1}H NMR spectra of **2** in benzene-d_6 and methanol-d_4 showed upfield signals at −43 and −41 ppm, respectively, characteristic of cationic diruthenium tetracarboxylate species.[2] Solid-state IR spectra of **2** contained carboxylate stretches corresponding to those for $\mathbf{1}^+$. The EPR signals for **2** in both coordinating and noncoordinating solvents occurred at ca. 1540 G, with effective g values[43] of 4.4, and are typical for $Ru_2(O_2CR)_4^+$ species.[12,13] In toluene, a second EPR signal at 3149 G (g = 2.14) is attributed to $TCNE^{-\bullet}$ coordinated to the diruthenium core. In the presence of methanol, the second EPR signal was shifted to 3374 G (g = 2.00), corresponding to the presence of free $TCNE^{-\bullet}$. This signal not only confirms the presence of the radical anion in **2** but indicates that $TCNE^{-\bullet}$ is readily displaced by coordinating solvents without cleaving the Ru−Ru bond. The C≡N stretches for **2** fall in the range seen for other species containing $TCNE^{-\bullet}$ (Table 3). A band seen at 1348 cm^{-1} in the IR spectrum of **2** is tentatively assigned to the C═C stretch of the radical anion $TCNE^{-\bullet}$. The fact that this stretch is seen in the IR indicates that $TCNE^{-\bullet}$ is not bound symmetrically. The high solubility of **2** suggests that $TCNE^{-\bullet}$ does not bridge between diruthenium units symmetrically or asymmetrically.

As the proposed structure indicates, $TCNE^{-\bullet}$ does not simply coordinate in the axial site but displaces a bridging equatorial carboxylate ligand from the $Ru_2(O_2CR)_4^+$ core. ^{1}H NMR spectra of **2** in aromatic solvents (Figure 10) showed two series of signals, one of which corresponded to $\mathbf{1}^+$. The second set contained broad signals with a chemical shift pattern similar to, but not as far upfield, as those seen for the axial carboxylate in $Ru_2(O_2CR)_5$,[2] suggesting that the displaced carboxylate ligand in **2** is not truly axial but occupies both axial and equatorial sites either as a chelating or bridging/chelating ligand. The ready displacement of the the carboxylate in methanol-d_4, indicated by the appearence of signals corresponding to uncoordinated octanoate, suggests that the carboxylate is chelating as in **I**. The presence of paramagnetically shifted signals in the ^{1}H NMR and EPR spectra indicate that the Ru−Ru bond remains intact and is not being cleaved to form mononuclear species.

A deficiency of TCNE results in a different product. When only $^1/_2$ equiv of TCNE was added to **1** in toluene,

(39) (a) Telser, J.; Drago, R. S. *Inorg. Chem.* **1986**, *25*, 2989. (b) Telser, J.; Drago, R. S. *Inorg. Chem.* **1984**, *23*, 2599.
(40) (a) Girolami, G. S.; Mainz, V. V.; Andersen, R. A. *Inorg. Chem.* **1980**, *19*, 805. (b) Cotton, F. A.; Lay, D. G. *Inorg. Chem.* **1981**, *20*, 935.
(41) Mountford, P.; Williams, J. A. G. *J. Chem. Soc., Dalton Trans.* **1993**, 877.
(42) Girolami, G. S.; Andersen, R. A. *Inorg. Chem.* **1981**, *20*, 2040.
(43) Pilbrow, J. R. *J. Magn. Reson.* **1978**, *31*, 479.

$[Ru_2(O_2C(CH_2)_6CH_3)_4]_2TCNE$ (**3**) precipitated immediately. The 2:1 product, **3**, was readily converted to the 1:1 species, **2**, by addition of TCNE. Spectroscopic studies suggest that **3** consists of $TCNE^{-\bullet}$ bridging two diruthenium units, one of which is oxidized and distorted as in **I**. The lack of a C═C stretch in the IR spectrum of **3** indicates that $TCNE^{-\bullet}$ is in a symmetrical environment while the shift of C≡N stretches to lower energy, which occurs when more electron density is transferred to TCNE, is consistent with $TCNE^{-\bullet}$ being coordinated to more diruthenium units. EPR studies suggest that $TCNE^{-\bullet}$ is more tightly bound to the dimetal centers in **3** than in **2**. Unlike **2**, the EPR spectrum of **3** in toluene/methanol showed no signal which could be attributed to free $TCNE^{-\bullet}$. When only $^1/_2$ equivalent of TCNE is present, only some of **1** is oxidized. The ^{1}H NMR spectrum of **3** in toluene-d_8 at 60 °C, although not very soluble, showed signals corresponding to both neutral and cationic diruthenium cores. The EPR spectrum of **3**, like $\mathbf{1}^+$, showed a signal at ca. 1540 G ($g = 4.4$), while the IR band at 1549 cm^{-1} corresponded to the asymmetric carboxylate stretch of **1**. Coordination of TCNE in **3** also disrupted the D_{4h} core of the diruthenium species, resulting in signals for uncoordinated octanoate in the ^{1}H NMR spectrum of **3** in methanol-d_4. In addition, the IR band at 1587 cm^{-1} may be indicative of a monodentate carboxylate. The presence of paramagnetically shifted signals in the ^{1}H NMR and EPR spectra are consistent with those seen for diruthenium tetracarboxylates, indicating that, despite the disrupted D_{4h} core, the Ru−Ru bond remains intact and is not being cleaved to form mononuclear species.

Redox Reactions with *p*-Benzoquinone. Benzoquinones may exist in one of three different oxidation states: the neutral benzoquinone (BQ), semiquinone ($SQ^{-\bullet}$), or the fully-reduced hydroquinone (HQ^{2-}). When reacted with $Ti(tol)_2$ (tol = toluene) or $Ge(N(SiMe_3)_2)_2$, *p*-benzoquinone and its derivatives undergo two-electron reductions to form hydroquinone-linked polymers.[44,45] Benzoquinones are not strong enough oxidants, however, to oxidize either $Rh_2(O_2CR)_4$ or $Mo_2(O_2CR)_4$ species and merely act as neutral bridges in the presence of these complexes. The dimolybdenum species are linked via both oxygen atoms in 9,10-anthraquinone in a relatively linear arrangement,[46] and their coordination is favored by the presence of electron-withdrawing O_2CCF_3 ligands at the dimetal core. $Rh_2(O_2CC(CH_3)_3)_4$ units are linked via one oxygen and a C═C bond of *p*-benzoquinone, in an asymmetric bridging mode.[47]

Even though the $Ru_2(O_2CR)_4$ species are much more easily oxidized than the molybdenum or rhodium species,[2] the oxidation does not occur without prior coordination of *p*-benzoquinone (BQ). The reactions of **1** with 1 equiv of BQ in toluene did not form polymeric quinone-bridged species at room temperature. ^{1}H NMR studies of **1** and BQ in toluene-d_8 at room temperature showed the broad signals of **1** without strongly-coordinated axial ligands[2] and relatively sharp unshifted BQ signals (Figure 11a). When the conditions were changed to favor coordination of BQ (the temperature was lowered or a large excess of BQ was used) evidence for coordination of BQ and oxidation of **1** was seen (eq 2). Solutions darkened

$$Ru_2(O_2CR)_4 + BQ \rightleftharpoons Ru_2(O_2CR)_4BQ \rightleftharpoons [Ru_2(O_2CR_4)]^+[SQ^{\bullet-}] \quad (2)$$

significantly. In the VT ^{1}H NMR spectra (Figure 11b,c), the presence of $\mathbf{1}^+$ is indicated by the extreme upfield signal. With 2 equiv of BQ, the conversion was complete at 12 °C, while, with 1 equiv, cooling to −10 °C was necessary. No signal for

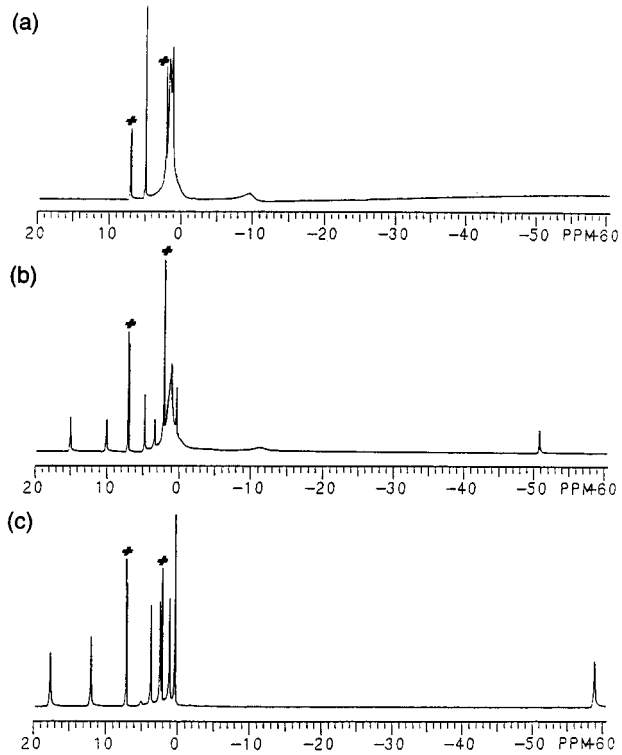

Figure 11. VT ^{1}H NMR spectra for **1** and *p*-benzoquinone at (a) 30 °C, (b) 10 °C, and (c) −10 °C in toluene-d_8. The resonances indicated by an asterisk arise from protio impurities in the solvent

a quinone species was seen, suggesting that the radical semiquinone ($SQ^{-\bullet}$), whose protons would relax too quickly to be seen by NMR, was formed. Reaction of **1** with an excess (>10 equiv) of BQ resulted in dark solutions at room temperature. Addition of hexanes lead to a dark solid, **4**, whose solid-state IR spectrum differed from those of **1** and $\mathbf{1}^+$, with a weak signal at 3031 cm^{-1} and other signals at 1332 and 794 cm^{-1}, indicative of coordinated quinone, presumably in a reduced form. Elemental analysis indicated that **4** contained a 1:1 ratio of diruthenium tetraoctanoate and quinone units.

The redox reaction is reversible. Warming of the ^{1}H NMR samples or dissolution of **4** simply gave spectra of **1** and free BQ. When BQ is coordinated to **1**, their relative redox potentials are apparently altered to favor the right side of the redox reaction in eq 2. Such a change in redox potential has been reported for the 2,3-dichloro-5,6-dicyano-*p*-benzoquinone 1−/2− redox couple when the ligand is coordinated to zinc tetraneopentoxyphthalocyanine.[48] Dissociation of **4** to $\mathbf{1}^+$ and $SQ^{-\bullet}$ changes the redox potentials back so that the left side of eq 2 is favored and **1** and BQ are re-formed.

In THF, the redox process described above is not operative. A sample of **1** with 1 equiv of BQ in THF-d_8 was cooled to −80 °C without any sign of $\mathbf{1}^+$ or even broadening of the BQ signal. Apparently THF is preventing the coordination of BQ and the reaction in eq 2. When **1** was reacted with tetrachloro-*p*-benzoquinone, a stronger oxidant,[49] in THF still no sign of redox was observed.

Since the redox reaction in eq 2 does not occur until after BQ is coordinated to **1**, coulombic attraction cannot favor initial

(44) Burch, R. R. *Chem. Mater.* **1990**, *2*, 633.
(45) Kobayashi, S.; Iwata, S.; Abe, M.; Shoda, S. *J. Am. Chem. Soc.* **1990**, *112*, 1625.
(46) Handa, M; Sono, H.; Kasamatsu, K.; Kasuga, K.; Mikuriya, M.; Ikenoue, S. *Chem. Lett.* **1992**, 453.
(47) Handa, M.; Takata, A.; Nakao, T.; Kasuga, K.; Mikuriya, M.; Kotera, T. *Chem. Lett.* **1992**, 2085.
(48) Fu, Y.; Fu, G.; Lever, A. B. P. *Inorg. Chem.* **1994**, *33*, 1038.
(49) Sasaki, K.; Kashimura, T.; Ohura, M.; Ohsaki, Y.; Ohta, N. *J. Electrochem. Soc.* **1990**, *137*, 2437.

coordination. However, once coordination and redox occurs the coulombic interactions would be expected to maintain the bond. The ready dissociation of **4** suggests that these interactions between charged species are not as stabilizing as first thought and that relatively weak, if any, π-interactions occur between Ru−Ru π^* and quinone π orbitals.

Conclusions

Reaction of pyrazine with $Ru_2(O_2C(CH_2)_6CH_3)_4$ (**1**) did lead to the formation of a polymeric species [**1**(pz)]$_n$. The solubility of [**1**(pz)]$_n$ is enhanced by the presence of the long carboxylate chains, and the length of the extended chain in noncoordinating solvents is concentration dependent. Although the species present in solution vary, the only species deposited from solutions, regardless of the solvent or ratio of **1**:pz, is [**1**(pz)]$_n$. This situation is favorable for processing should the species have industrial applications. The polymer has an extended π-system, but recently reported solid-state magnetic studies on similar species showed that it results in only weak antiferromagnetic interactions.[7,50] Our solid-state studies showed that pyrazine dissociates from [**1**(pz)]$_n$ at high temperatures, meaning that the polymer could only be used for applications under 140 °C.

The presence of the C≡N group in 4-cp enhanced the π-interactions of the pyridine ring with **1**. Although solution studies suggest that the C≡N group does coordinate to **1**, the interaction is very weak and no polymers were isolated. The isolated **1**(4-cp)$_2$ units could perhaps be linked together by other species which form strong bonds with nitriles.

TCNE undergoes a redox reaction with **1** and induces structural rearrangement of the diruthenium tetracarboxylate core. Such rearrangement without Ru−Ru bond cleavage is unprecedented. We have been unable to determine the exact nature of the species, but it appears to have at least one carboxylate ligand displaced from the equatorial sites of the diruthenium core. Further investigations may lead to an understanding of the mechanism for Ru−Ru bond cleavage.

p-Benzoquinone also undergoes a redox reaction with **1** but only after coordination to the axial site. Unlike the reaction with TCNE, the reaction with *p*-benzoquinone does not appear to involve ligand migration. Thus, **4** is thought to be the anticipated axially-coordinated anionic/cationic system. Unfortunately, the species does not possess the expected stability and returns to **1** and *p*-benzoquinone when dissolved.

In these studies we have used the information gained in previous studies of **1**[2] to examine its reactions with various linking groups. The solubility of the octanoate derivative allowed solution studies, providing much information, but at the same time precluded the formation of single crystals for X-ray studies. Attempts involving the butyrate and acetate derivatives have not led to crystals either; thus we have not been able to obtain specific data for the Ru−N distances or the geometry of the TCNE adducts. The solution studies have indicated that neither enhanced π-interactions nor ionic interactions are of sufficient strength to counteract the lability of axial ligands on $Ru_2(O_2CR)_4$ units and form robust polymers.

Experimental Section

All compounds were handled under argon or nitrogen using Schlenk techniques and gloveboxes. Toluene, hexanes, THF, and diethyl ether were distilled under nitrogen from sodium or potassium with benzophenone, and dichloromethane was distilled from calcium hydride. All solvents were stored over molecular sieves. Anhydrous methanol, acetonitrile, and diglyme were bought from Aldrich, degassed, and stored over molecular sieves. ^{1}H NMR spectra were recorded on a Varian XL-300 spectrometer at 23 °C unless stated otherwise, UV/visible spectra on a HP8452A diode array spectrophotometer with UV/visible operating software 89531A, IR spectra on a Nicolet 510P FT-IR spectrophotometer, and EPR spectra on a Bruker ESP300 spectrometer with a Hewlett-Packard 5350B microwave frequency counter and an Oxford liquid He cryostat and temperature controller. Elemental analyses were performed by Oneida Research Services. DSC experiments were performed on a DuPont 910 differential scanning calorimeter under N_2 flow at a heating rate of 5 °C/min.

$Ru_2(O_2C(CH_2)_6CH_3)_4$ [2] and $Ru_2(O_2C(CH_3)_6CH_3)_4Cl$ [2] were synthesized via literature methods. Pyrazine, pyridine, 4-cyanopyridine, and TCNE were purchased from Aldrich. With the exceptions of 4-cyanopyridine, which was recrystallized from diethyl ether, and TCNE, which was sublimed before use, all were used without further purification.

Extended Hückel MO calculations were carried out by using the EHMACC program.[51] On the basis of the structural data for $Ru_2(O_2CMe)_4(H_2O)_2$[52] the distances and angles for $Ru_2(O_2CH)_4$, idealized to D_{4h}, were Ru−Ru = 2.262 Å, Ru−O = 2.066 Å, C−O = 1.306 Å, C−H = 1.08 Å, Ru−O−C = 120°, and O−C−H = 120°. The geometry of pyrazine was taken from the structure of $[Ru(NH_3)_5]_2$-pz^{4+},[16b] where N−C = 1.353 Å, C−C = 1.363 Å, C−H = 1.08 Å, C−N−C = 113°, N−C−C = 123°, and C−C−H = 118.5°. Ru−N distances of 2.4 Å were used.

Synthesis of [1(pz)]$_n$. Via syringe 16.2 mL of a 5.00×10^{-2} M toluene solution of pyrazine (0.810 mmol) was added to **1** (0.625 g, 0.807 mmol) dissolved in toluene (10 mL). An immediate color change from brown to purple was observed. Cooling to −20 °C resulted in purple powder, which was filtered out and washed with hexanes. Yield: 0.439 g (64%). Anal. Calcd for $Ru_2O_8C_{36}H_{64}N_2$: C, 50.57; H, 7.55; N, 3.28. Found: C, 50.69; H, 7.78; N, 2.81. IR (KBr, cm^{-1}): 3095 w, 2955 s, 2926 vs, 2851 s, 1550 vs, 1481 m, 1454 s, 1427 vs, 1377 w, 1354 w, 1317 m, 1281 w, 1259 w, 1159 m, 1126 s, 1113 w, 1041 s, 815 m, 801 w, 726 m, 716 m, 667 m.

Synthesis of 1(4-cp)$_2$. 4-cp (0.0511 g, 0.490 mmol) in toluene (3 mL) was added to **1** (0.190 g, 0.245 mmol) in toluene (15 mL). The solution immediately turned dark red. Hexanes (70 mL) were added. Upon cooling to −20 °C, precipitate formed. Initial batches were sludgy and difficult to isolate. Subsequent batches were filtered and washed with hexanes. Anal. Calcd for $Ru_2O_8C_{44}H_{68}N_4$: C, 53.75; H, 6.97; N, 5.70. Found: C, 53.35; H, 7.08; N, 5.72. IR (KBr, cm^{-1}): 3108 w, 3044 w, 2953 s, 2922 vs, 2851 s, 2238 m, 2205 br w, 1603 m, 1560 vs, 1491 m, 1462 s, 1429 vs, 1417 vs, 1315 m, 1304 w, 1261 w, 1223 m, 1111 m, 1067 m, 1007 m, 822 s, 723 m, 662 m, 556 s.

Synthesis of Ru(O$_2$C(CH$_2$)$_6$CH$_3$)$_2$(4-cp)$_4$. 4-cp (0.135 g, 1.30 mmol) in toluene (10 mL) was added to **1** (0.05 g, 0.06 mmol) in toluene (10 mL). The solution was stirred for 10 days. The volume of solution was reduced to 5 mL *in vacuo*. Hexanes (70 mL) were added. Upon cooling to −20 °C, precipitate formed which was isolated by filtration. Yield: 69%. ^{1}H NMR (benzene-d_6, δ): 8.79 (1H), 8.43 (2H), 8.07 (1H), 6.29 (2H), 6.2 (1H), 2.56 br (1H), 2.41 m, (1H), 1.8 br (1H), 1.72 m (1H), 1.23 v br (8H), 0.88 br (3H). IR (KBr, cm^{-1}): 3038 w, 2955 m, 2926 s, 2855 m, 2232 s, 1616 s, 1605 vs, 1588 vs, 1487 m, 1420 m, 1369 s, 1219 m, 1194 m, 1101 m, 1015 s, 835 s, 565 m, 488 w. UV/visible (toluene, 6.2×10^{-5} M): 488 nm (19 200 M^{-1} cm^{-1}), 540 (sh) nm (14 600 M^{-1} cm^{-1}).

UV/Visible Titrations. Mole Ratio Method.[27b] An 8.00×10^{-4} M solution of **1** in toluene was prepared. Aliquots (10 mL) were pipetted into 25-mL volumetric flasks. A 2.00×10^{-3} M solution of the ligand (pyrazine or 4-cp) was prepared, and 1, 2, 3, 4, 6, and 8 mL aliquots were added to the samples of **1** to give solutions of 4:1, 2:1,

(50) Cukiernik, F. D.; Giroud-Godquin, A.-M.; Maldivi, P.; Marchon, J.-C. *Inorg. Chim. Acta* **1994**, *215*, 203.

(51) EHMACC, an Extended Hückel Molecular, Crystal and Properties Package, QCPE 571, was obtained from the Quantum Chemistry Program Exchange, Indiana University, Bloomington, IN 47405.

(52) Lindsay, A. J.; Wilkinson, G.; Motevalli, M.; Hursthouse, M. B. *J. Chem. Soc., Dalton Trans.* **1985**, 2321.

(53) Gross, R.; Kaim, W. *Angew. Chem., Int. Ed. Engl.* **1987**, *26*, 251.

(54) Miller, J. S.; Calabrese, J. C.; McLean, R. S.; Epstein, A. J. *Adv. Mater.* **1992**, *4*, 498.

(55) Beck, W.; Schlodder, R.; Lechler, K. H. *J. Organomet. Chem.* **1973**, *54*, 303.

3:2, 1:1, 2:3, and 1:2 ratios of **1**:L. Each solution was diluted to 25 mL. For ratios smaller than 1:2 either a more concentrated solution of ligand was prepared or the appropriate amount of solid was added.

Absorbance values (A_{obs}) for each solution at the selected wavelengths were measured. A_M, the absorbance values expected if the ligand did not react, were taken from the spectrum of 10 mL of the solution of **1** diluted to 25 mL. $A_{obs} - A_M$ for each wavelength and mole ratio were plotted vs mole ratio of the ligand [$moles_L/moles_M$]. A_L was zero at all wavelengths used.

Method of Continuous Variations.[27] Isomolar solutions (3.5×10^{-4} to 5.1×10^{-4} M) of **1** and the ligand (pyrazine and 4-cp) were prepared. The solutions using volume ratios from 1:9 to 9:1 mL were prepared, and absorbance values (A_{obs}) at selected wavelengths were measured. A_M was calculated ($A = lM\epsilon$) using 1-cm path length, the appropriate concentration of **1**, and molar absorptivities calculated from the stock solution of **1**. $A_{obs} - A_M$ for each wavelength and mole ratio were plotted vs mole fraction of the ligand [$moles_L/(moles_M + moles_L)$]. Once again A_L was zero and not included in the correction of A_{obs}.

Solution IR. A dichloromethane solution 1.83×10^{-2} M in **1** was prepared. Aliquots of 1 mL were combined with the appropriate amount of 4-cp. The IR spectra of these solutions were compared to those of solutions of the free ligand.

$[Ru_2(O_2C(CH_2)_6CH_3)_4TCNE]_n$ (2). A solution of TCNE (0.0273 g, 0.213 mmol) in toluene (10 mL) was added to a solution of **1** (0.1654 g, 0.213 mmol) in toluene (15 mL). A dark precipitate was seen upon addition of half of the TCNE solution, but upon addition of the rest of the TCNE solution it redissolved to form a dark red solution. After the solution was stirred several hours, the volume was reduced to 5 mL. Hexanes were added, and the solution was stored at −20 °C. The precipitate was isolated by filtration and washed with hexanes. Yield: 0.1148 g (60%). Anal. Calcd for $Ru_2O_8C_{38}H_{60}N_4$: C, 50.54; H, 6.70; N, 6.21. Found: C, 50.43; H, 6.48; N, 5.94. IR (KBr, cm^{-1}): 2959 s, 2928 vs, 2857 s, 2247 s, 2234 m, 2224 s, 1455 vs, 1431 vs, 1418 vs, 1348 s, 1318 m, 727 w, 683 m, 679 m. ^{1}H NMR (benzene-d_6, δ): 16.5 (CH_2(3)), 10.6 (CH_2(4)), 5.7 (CH_2(5)), 4.4 (CH_2(6)), 3.3 (CH_2(7)), 2.2 (CH_3(8)), 1.6, 1.2, 0.7 (br), 0.3 (br), −0.5 (br), −29 (v br), −43 (CH_3(2)). ^{1}H NMR (methanol-d_4, δ): 15.7 (CH_2(3)), 12.7 (CH_2(4)), 6.6 (CH_2(5)), 5.0 (CH_2(6)), 3.5 (CH_2(7)), 2.3, 2.0 (CH_3(8)), 1.5, 1.2, 0.8, −41 (CH_2(2)).

$[Ru_2(O_2C(CH_2)_6CH_3)_4]_2TCNE$ (3). A solution of TCNE (0.091 g, 0.071 mmol) in toluene (5 mL) was added with stirring to a solution of **1** (0.110 g, 0.142 mmol). The dark precipitate, which formed immediately, was filtered out and washed with hexanes. Yield: 0.098 g (82%). Anal. Calcd for $Ru_4O_{16}C_{70}H_{120}N_4$: C, 50.10; H, 7.21; N, 3.34. Found: C, 50.58; H, 7.31; N, 3.97. IR (KBr, cm^{-1}): 2957 s, 2928 vs, 2855 s, 2228 s, 2219 s, 1591 s, 1547 m, 1458 vs, 1431 vs, 1418 vs, 1312 m, 725 w, 671 m. ^{1}H NMR (toluene-d_8, 60 °C, δ): 13.0, 8.5, 5.0, 4.0, 3.1, 2.1, 1.6, 1.2, 1.1, 0.9, 0.3, −7 (v br), −23, −37. ^{1}H NMR (methanol-d_4, δ): 16.3, 15.4, 12.5, 11.9, 6.8, 5.2, 4.2, 3.7, 3.1, 2.2, 2.1, 1.8, 1.5, 1.2, 0.8, −39, −40.

EPR Spectra of 2 and 3. Spectra of 0.002 M solutions were taken at 4.9 K. The sample of **2** in toluene (9.439 GHz) gave signals with effective g values of 4.36 and 2.14. In a 5/1 mixture of toluene/methanol **2** gave two signals with effective g values of 4.37 and 2.00 (9.441 GHz) and **3** gave one signal with an effective g value of 4.39 (9.438 GHz).

Reaction of 1 + *p*-Benzoquinone. A solution of *p*-benzoquinone (0.0138 g, 0.128 mmol) in toluene (2 mL) was added to **1** (0.099 g, 0.128 mmol) dissolved in toluene (5 mL). The solution remained brown. When cooled to −20 °C, a very dark solution resulted. Warming to room temperature caused a return of the brown color and within several hours, a brown precipitate had formed. The precipitate was filtered out and dried. IR and ^{1}H NMR (benzene-d_6 and methanol-d_4) spectra were identical to those of **1**. Removal of solvent from the filtrate left a brown residue which contained $\mathbf{1}^+$, octanoate, and quinone. ^{1}H NMR (methanol-d_4, δ): 15.8 (CH_2(3)), 12.3 (CH_2(4)), 6.6, 6.54 (CH_2(5)), 4.92 (CH_2(6)), 3.49 (CH_2(7)), 2.06 (CH_3(8)), 1.19, 0.86, −40 (CH_2(2)).

Reaction of 1 + Excess *p*-Benzoquinone To Form $[\mathbf{1}^+][SQ^{-\bullet}]$ (4). A solution of *p*-benzoquinone (0.139 g, 1.29 mmol) in toluene (5 mL) was added to **1** (0.050 g, 0.065 mmol) dissolved in toluene (10 mL). The solution turned dark immediately. The volume was reduced to 5 mL. Hexanes (70 mL) were added and the solution cooled to −20 °C. The precipitate was filtered out and washed with hexanes. Anal. Calcd for $Ru_2O_{10}C_{38}H_{64}$: C, 51.68; H, 7.31. Found: C, 51.52; H, 7.15. Found: IR (KBr, cm^{-1}): 3031 w, 2961 m, 2920 s, 2849 m, 2738 w, 1653 w, 1597 w, 1559 m, 1487 vs, 1460 vs, 1416 vs, 1332 s, 996 m, 851 m, 794 vs, 723 w, 667 m, 519 w, 476 w, 443 m.

Acknowledgment. We thank the National Science Foundation for support, Johnson Matthey for a generous loan of ruthenium trichloride, and Michael Wemple for assistance in obtaining EPR and ^{2}H NMR data.

Supporting Information Available: Tables of absorption data for the titration of **1** with both pz and 4-cp in toluene (2 pages). Ordering information is given on any current masthead page.

IC970173Y